CHAPTER III

GEOCHEMISTRY

Treatment of Analytical Data

Raw analytical data of standard chemical composition of most natural basaltic rocks are recommended recently by numbers of literatures to be adjusted for the effect of oxidation and for the uniformity of the results.

Two main adjustments have been proposed (Irvine and Baragar, 1971):

(1) Adjust the ratio Fe_2O_3/FeO if it appears to have been changed. The aim in making this adjustment should be to come as close as possible to the primary composition of the rock. The significant effect of Fe_2O_3 content will be on the norm which hence to some extent nomenclature, and on other important petrological parameters such as $100 \times Mg/(Mg+Fe^{2+})$ ratio or Mg-value (Irving and Green, 1976). Irvine and Baragar (1971) set the upper limit of Fe_2O_3 according to the equation $\%Fe_2O_3 = \%TiO_2 + 1.5$, which based on the observations that Fe_2O_3 and TiO_2 are generally have similar trends of variation in unaltered volcanic series. No change will be made on the analysis value, unless it is greater, then the excess is converted to FeO. The result of this adjustment would yield a more undersaturated norm.

(2) Recalculate analysis to 100% without H_2O or CO_2. This adjustment will simply place all comparisons on the same basis. In this study the volatiles are expressed in term of H_2O^- and loss on ignition. Even though these measurements are not generally of interest in respect to magmatic composition, they are still significant chemical indicators of the state of alteration of the rocks.

The Bo Phloi Basalt contains slightly high contents of H_2O^- (0.46-1.12 wt%), loss on ignition (1.92-4.56 wt%) and Fe_2O_3 (2.99-4.69 wt%). Petrographically, it shows evidences of oxidation, e.g. iddingsite and hematite, so the Fe_2O_3/FeO ratio is set on the uppermost limit of 0.6 (Irvine and Baragar, 1971.)

Bo Phloi Basalt

The adjusted chemical analyses and CIPW norms of twenty Bo Phloi volcanic rocks are presented on Table 1. Table 2 gives the average, range and standard deviation of the major oxides whereas Table 3 illustrates the chemical parameters.

The rather small distribution of the Bo Phloi Basalt has confined the variation of rocks both mineralogically and geochemically into a limited range. Nonetheless, when oxides of other elements are plotted against SiO_2, the contents of TiO_2, Al_2O_3, total FeO, MgO, CaO, K_2O and P_2O_5 tend to decrease and Na_2O tends to increase with increasing SiO_2 content (Figure 18). Two additional variation diagrams of oxides against solidification index (SI = MgO x 100/(MgO + FeO + Fe_2O_3 + Na_2O + K_2O)

Table 1 Major element chemical data and CIPW weight percent norms for the Bo-Phloi Basalt

	T79-1-2	T79-1-4	T79-1-6	T79-2-1	T79-2-3
SiO_2	48.08	47.09	46.65	49.47	51.16
TiO_2	1.88	1.88	2.34	2.04	1.84
Al_2O_3	15.59	15.58	15.68	16.52	16.21
Fe_2O_3	3.46	3.45	3.91	3.59	3.41
FeO	5.72	6.23	6.52	6.23	5.68
MnO	0.19	0.17	0.19	0.18	0.16
MgO	7.88	8.19	7.70	6.19	5.55
CaO	9.09	9.44	9.29	8.09	8.35
Na_2O	3.92	3.91	3.90	4.76	5.03
K_2O	3.31	3.26	2.84	2.04	1.84
P_2O_5	0.84	0.78	0.95	0.87	0.75
Cr_2O_3	0.02	0.02	0.02	0.02	0.02
Fe_2O_3/FeO	0.61	0.55	0.60	0.58	0.60
100 $Mg/Mg+Fe^{2+}$	71.06	70.00	67.73	63.90	63.59
Original sum	98.44	98.81	98.89	100.06	99.18
Nat. Fe_2O_3/FeO	0.73	0.88	0.65	0.82	0.91
H_2O^-	0.90	0.85	0.83	0.73	0.83
Loss on Ignition	2.49	2.89	2.69	2.68	2.65
or	19.56	19.26	16.78	12.05	10.87
ab	13.88	9.68	14.29	29.53	33.91
an	15.17	15.33	16.93	17.68	16.22
ne	10.45	12.68	10.14	5.82	4.69
di	19.46	21.08	18.41	13.41	16.29
ol	10.90	11.55	11.20	10.36	7.82
mt	5.02	5.00	5.67	5.21	4.94
il	3.57	3.57	4.44	3.87	3.49
ap	1.95	1.81	2.25	2.02	1.74
cm	0.03	0.03	0.03	0.03	0.03

Table 1 (continued)

	T79-2-4	T79-3-1	T79-3-2	T79-3-3	T79-4-1
SiO_2	47.39	50.15	50.27	47.71	48.27
TiO_2	2.27	1.94	1.96	1.98	2.34
Al_2O_3	14.75	14.58	14.43	15.94	16.18
Fe_2O_3	3.94	3.50	3.07	3.31	3.75
FeO	6.77	6.23	6.28	6.07	5.93
MnO	0.19	0.19	0.17	0.17	0.17
MgO	7.39	8.09	8.21	7.61	7.70
CaO	8.91	8.01	8.10	9.76	9.01
Na_2O	4.75	4.34	4.54	4.35	3.86
K_2O	2.77	1.94	1.96	2.30	1.99
P_2O_5	0.92	0.98	0.96	0.76	0.75
Cr_2O_3	0.03	0.04	0.04	0.04	0.04
Fe_2O_3/FeO	0.57	0.56	0.49	0.55	0.63
100 $Mg/Mg+Fe^{2+}$	65.82	69.79	70.10	69.23	69.70
Original sum	98.65	99.52	100.34	100.51	99.83
Nat. Fe_2O_3/FeO	0.67	0.65	0.49	0.55	0.63
H_2O^-	0.59	0.73	0.75	0.79	0.76
Loss on Ignition	2.63	2.54	2.35	2.46	3.30
or	16.37	11.46	11.58	13.59	11.76
ab	15.77	31.90	30.68	16.66	24.70
an	10.74	14.57	13.21	17.17	20.94
ne	13.23	2.61	4.19	10.91	4.31
di	21.96	14.98	16.55	20.99	14.98
ol	9.80	13.37	13.33	10.29	11.61
mt	5.71	5.07	4.45	4.80	5.44
il	4.31	3.68	3.72	3.76	4.44
ap	2.13	2.27	2.22	1.76	1.74
cm	0.04	0.06	0.06	0.06	0.06

Table 1 (continued)

	T79-4-2	T79-4-3	T79-5-1	T79-5-4	T79-6-1
SiO_2	47.90	48.45	48.86	48.00	50.34
TiO_2	2.01	2.26	1.88	2.03	2.03
Al_2O_3	15.51	16.26	16.19	16.10	15.29
Fe_2O_3	3.58	3.84	3.44	3.61	3.58
FeO	6.08	6.61	6.15	6.54	5.81
MnO	0.19	0.19	0.18	0.19	0.18
MgO	7.23	7.45	7.54	7.24	6.73
CaO	10.09	7.98	7.76	9.65	8.61
Na_2O	3.94	3.89	4.12	3.63	4.32
K_2O	2.58	1.99	3.00	2.11	2.31
P_2O_5	0.86	0.99	0.86	0.89	0.79
Cr_2O_3	0.02	0.07	0.02	0.02	0.02
Fe_2O_3/FeO	0.59	0.58	0.56	0.55	0.62
100 $Mg/Mg+Fe^{2+}$	67.80	66.79	68.50	66.42	67.34
Original sum	99.48	99.32	98.80	100.57	99.91
Nat. Fe_2O_3/FeO	0.67	0.58	0.76	0.88	0.80
H_2O^-	0.69	0.60	0.46	1.12	0.60
Loss on ignition	2.94	3.81	1.92	4.56	2.65
or	15.25	11.76	17.73	12.47	13.65
ab	16.53	29.42	21.85	22.23	28.81
an	17.06	21.08	16.82	21.40	15.51
ne	9.11	1.89	7.05	4.60	4.19
di	21.98	9.70	12.84	16.55	17.60
ol	9.15	13.96	13.13	11.58	9.34
mt	5.19	5.57	4.99	5.23	5.19
il	3.82	4.29	3.57	3.85	3.85
ap	2.04	2.34	1.99	2.06	1.83
cm	0.03	0.07	0.03	0.03	0.03

Table 1 (continued)

	T79-6-3	T79-6-6	T79-7-3	T79-7-4	T79-7-7
SiO_2	47.59	48.61	47.19	48.59	48.53
TiO_2	2.05	2.32	1.94	2.28	2.27
Al_2O_3	16.25	16.38	16.36	16.37	16.70
Fe_2O_3	3.60	3.88	3.50	3.49	3.70
FeO	6.10	6.05	6.34	5.83	6.00
MnO	0.15	0.18	0.18	0.18	0.20
MgO	8.04	7.32	7.49	7.41	7.49
CaO	8.57	7.35	7.61	8.09	8.01
Na_2O	4.08	4.94	5.18	4.69	3.84
K_2O	2.61	2.10	3.29	2.24	2.36
P_2O_5	0.94	0.85	0.89	0.80	0.87
Cr_2O_3	0.02	0.02	0.02	0.02	0.03
Fe_2O_3/FeO	0.59	0.55	0.55	0.60	0.62
100 $Mg/Mg+Fe^{2+}$	70.07	68.42	67.88	69.43	68.89
original sum	100.25	100.27	99.52	100.02	99.71
Nat. Fe_2O_3/FeO	0.86	0.94	0.57	0.60	0.62
H_2O^-	0.91	0.89	0.93	0.72	0.74
Loss on ignition	2.46	2.93	2.37	2.81	2.68
or	15.42	12.41	19.44	13.24	13.95
ab	19.15	27.85	13.16	24.57	26.39
an	18.32	16.32	11.67	17.00	21.36
ne	8.33	7.55	16.61	8.19	3.30
di	14.39	11.61	16.22	14.25	10.11
ol	13.07	12.22	12.03	11.47	13.16
mt	5.22	5.63	5.07	5.06	5.36
il	3.89	4.41	3.68	4.33	4.31
ap	2.18	1.97	2.06	1.85	2.02
cm	0.03	0.03	0.03	0.03	0.04

Table 2 Average, range and standard deviation of major oxides for the Bo-Phloi Basalt.

(wt %)	Range	Std.dev.	Average 1*	2*	3*
SiO_2	46.65 - 51.16	1.32	48.44	46.7	47.9
TiO_2	1.84 - 2.34	0.17	2.08	2.7	3.4
Al_2O_3	14.43 - 16.70	0.64	15.81	15.1	15.9
Fe_2O_3	3.07 - 3.94	0.45	3.64		4.9
FeO	5.68 - 6.77	0.49	6.05	11.7**	7.6
MgO	5.55 - 8.21	0.63	7.60	7.7	4.8
CaO	7.61 - 10.09	0.73	8.58	9.9	8.0
Na_2O	3.63 - 5.18	0.45	4.29	3.2	4.2
K_2O	1.84 - 3.31	0.46	2.44	1.2	1.5
P_2O_5	0.75 - 0.99	0.07	0.86		0.7
MnO	0.15 - 0.20	0.01	0.18		0.2
Cr_2O_3	0.02 - 0.07	0.01	0.03		

1* average Bo-Phloi Basalt

2* average alkali olivine basalts , Schwarzer and Rogers (1974)

3* average hawaiites, Irvine and Baragar (1971)

** Total iron as FeO

Table 3 Chemical parameters

	T79-1-2	T79-1-4	T79-1-6	T79-2-1	T79-2-3
Mafic index	53.81	54.71	57.53	61.34	62.09
Felsic index	44.30	43.16	42.05	45.70	45.14
Differentiation index	43.89	41.62	41.21	47.41	49.47
Solidification index	32.44	32.71	31.66	27.14	25.80
Mg-value	71.06	70.00	67.73	63.90	63.59
Normative color index	38.95	41.21	39.72	32.86	32.55
100 An/(An+Ab')	32.65	33.22	35.18	31.06	27.99
100 An/(An+Ab)	52.22	61.29	41.21	41.88	32.55
K_2O : Na_2O	0.84	0.83	0.73	0.43	0.37

	T79-4-2	T79-4-3	T79-5-1	T79-5-4	T79-6-1
Mafic index	57.19	58.52	55.98	58.37	58.25
Felsic index	39.25	42.42	47.85	37.30	43.50
Differentiation index	40.89	43.07	46.63	39.29	46.66
Solidification index	30.88	31.25	31.09	31.30	29.58
Mg-value	67.80	66.79	68.50	66.42	67.34
Normative color index	40.14	33.52	34.53	37.32	35.99
100 An/(An+Ab')	34.98	39.29	33.36	29.44	27.61
100 An/(An+Ab)	50.79	41.74	43.49	49.05	34.99
K_2O : Na_2O	0.65	0.51	0.73	0.58	0.53

Table 3 (continued)

	T79-2-4	T79-3-1	T79-3-2	T79-3-3	T79-4-1
Mafic index	59.17	54.60	53.05	55.21	55.70
Felsic index	45.77	43.94	44.52	40.52	39.37
Differentiation index	45.37	45.98	46.45	41.17	40.77
Solidification index	28.84	33.57	34.12	32.19	33.15
Mg-value	65.82	69.79	70.10	69.23	69.70
Normative color index	41.79	37.11	38.05	39.84	36.48
100 An/(An+Ab')	22.12	28.67	25.97	33.00	39.64
100 An/(An+Ab)	40.15	31.35	31.10	50.75	45.88
K_2O : Na_2O	0.58	0.45	0.43	0.53	0.52

	T79-6-3	T79-6-6	T79-7-3	T79-7-4	T79-7-7
Mafic index	54.68	57.57	56.78	55.71	56.43
Felsic index	43.84	48.92	52.67	46.14	43.63
Differentiation index	42.90	47.82	49.22	45.99	43.64
Solidification index	32.91	30.14	29.03	31.32	32.02
Mg-value	70.07	68.42	67.88	69.43	68.89
Normative color index	36.57	33.87	37.01	35.11	32.94
100 An/(An+Ab')	32.09	23.48	32.25	25.73	30.43
100 An/(An+Ab)	48.89	36.95	47.00	40.89	44.73
K_2O : Na_2O	0.64	0.43	0.64	0.481	0.61

Mafic index (M.I.) = 100 $(FeO+Fe_2O_3)/(FeO+Fe_2O_3+MgO)$

(Wagner and Deer, 1939)

Felsic index (F.I.) = 100 $(Na_2O+K_2O)/(CaO+Na_2O+K_2O)$

(Simpson, 1954)

Differentiation index (D.I.) = normative Q+Or+Ab+Ne+Ks+Lc

(Thornton and Tuttle, 1960)

Solidification index (S.I.) = 100 $MgO/(MgO+FeO+Fe_2O_3+Na_2O+K_2O)$

(Kuno, 1969)

Mg-value = 100 Mg / $(Mg+Fe^{2+})$

(Wagner and Deer, 1939)

Normative color index = Ol+Opx+Cpx+Mt+Il+hm

(Irvine and Baragar, 1971)

Normative plagioclase composition = 100 An/(An+Ab)

and in Irvine and Baragar (1971) = 100 An/(An+Ab') ; Ab' = Ab+5/3 Ne

(Kuno, 1969) and MgO are presented in Figure 19 and Figure 20, respectively. The characteristic features of these two variation diagrams are quite similar, namely, SiO_2, Na_2O and Al_2O_3 increase and P_2O_5, TiO_2, CaO, total FeO, MgO and K_2O decrease with decreasing SI and MgO. These plots indicate tendency for a process of differentiation (Saggerson and Williams, 1964).

Compositional plots of the Bo-Phloi Basalt in AFM Triangular variation diagram (Figure 21) shows relatively low in FeO and high in $Na_2O + K_2O$ and MgO in compared with other corundumless basalts in Thailand which are mostly alkali basalts (Barr and Macdonald, 1978 and Vichit et.al., 1978), and with alkali basalts from four different places outside the country (Coombs and Wilkinson, 1969). The relatively low total iron is also shown in Figure 22 and Table 2. The relatively high contents of the alkali is principally reflected from the high contents of K_2O. Figure 23 shows the relationship between K_2O and Na_2O. The K_2O contents are positively correlated to the contents of Na_2O and the K_2O/Na_2O ratios are bounded in between 1/3 -1. However, the majority of K_2O/Na_2O ratios are higher than 1/2.

The normative color index of the Bo-Phloi Basalt ranges from 32 to 42 (average 36.6). This range of color index together with the low silica content (46.65 - 51.16 wt%, average 48.4 wt%) suggests the rocks are basaltic composition. Moreover, the presence of silica undersaturated minerals in the norm, i.e., nepheline (2.6 - 16.6 wt%) and olivine (7.8 - 13.4 wt%) and the absence of hypersthene norm

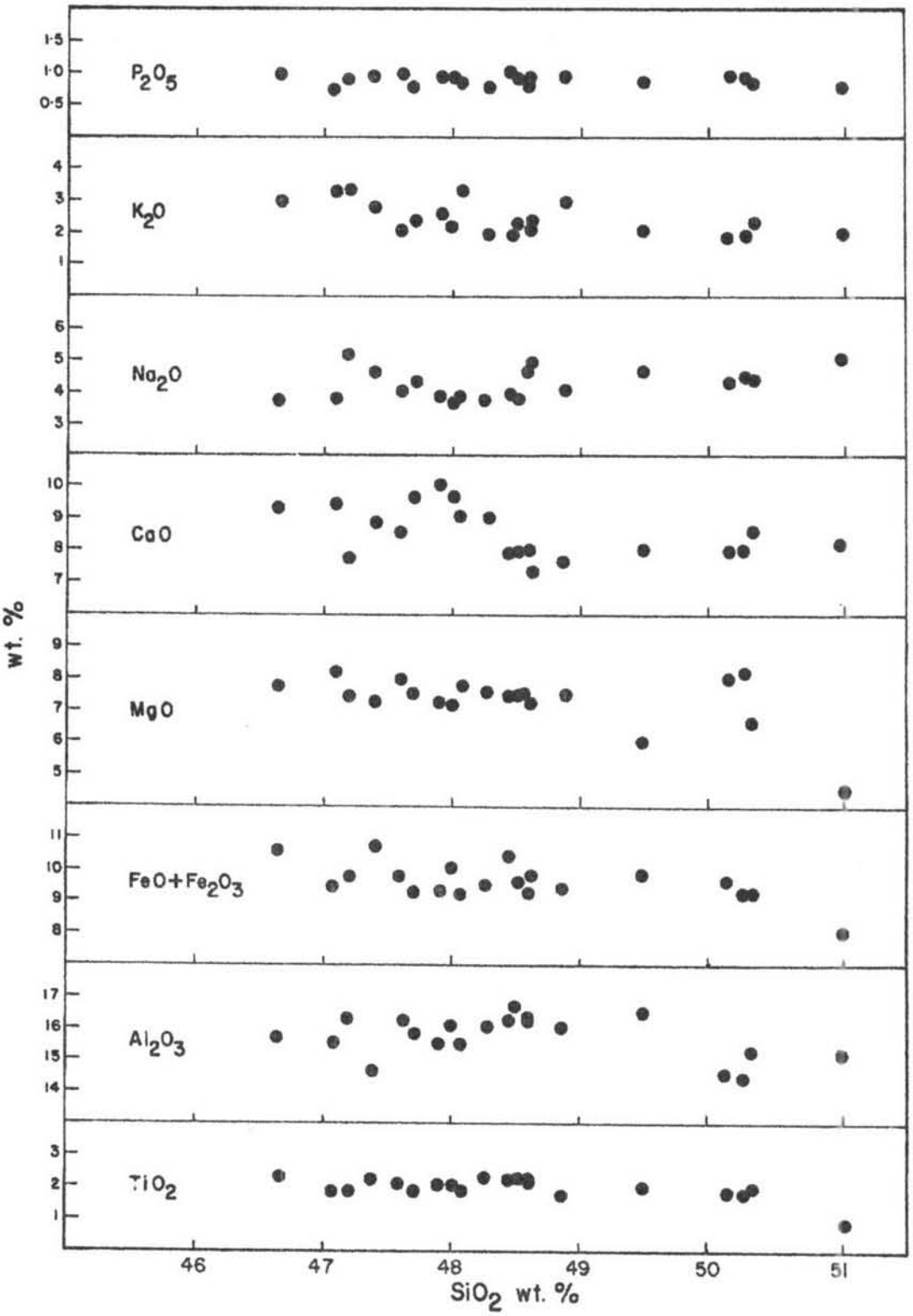

Figure 18 *Silica variation diagram for the Bo-Phloi Basalt.*

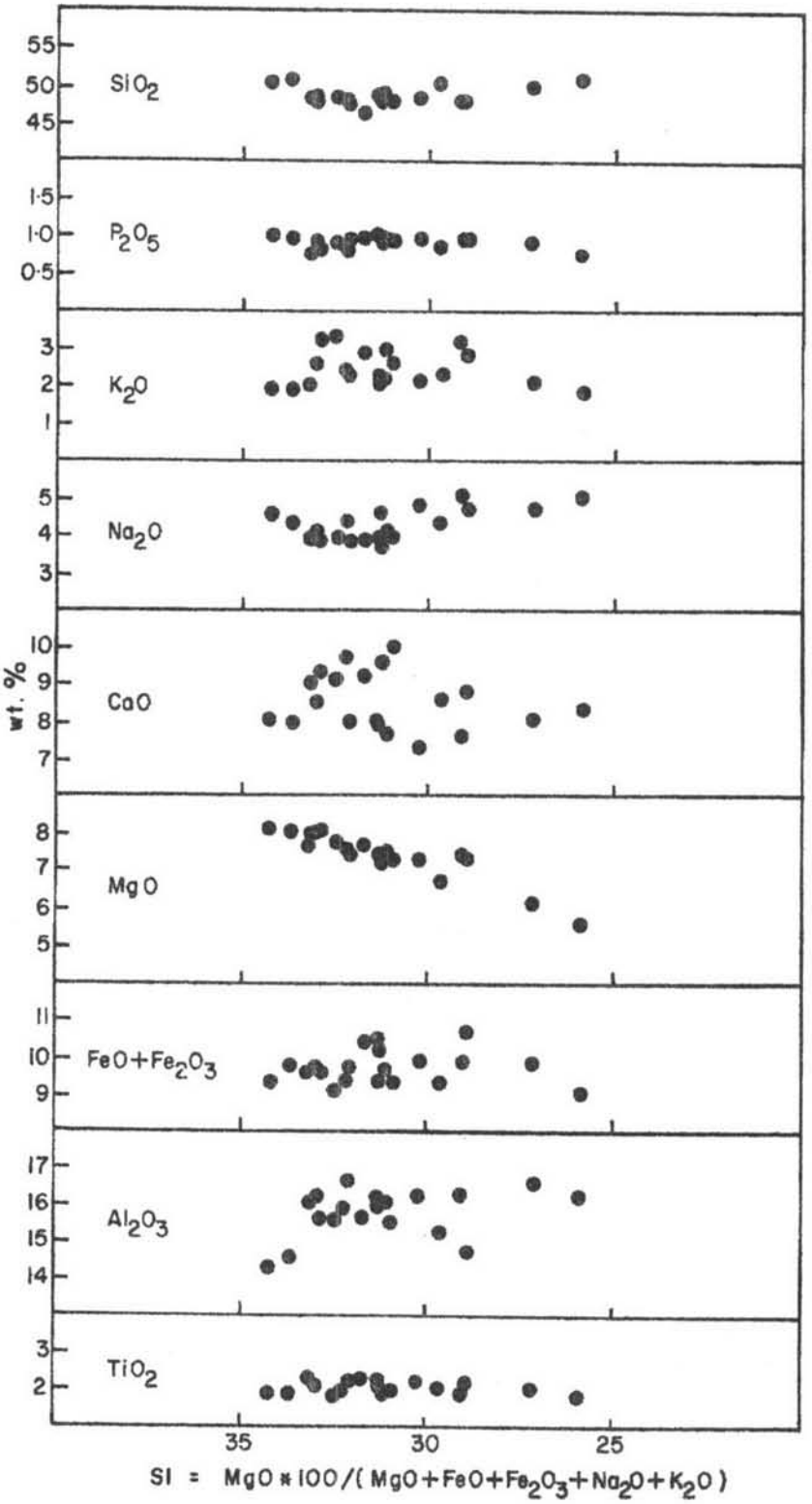

Figure 19 *Solidification index (SI) diagram for the Bo-Phloi Basalt.*

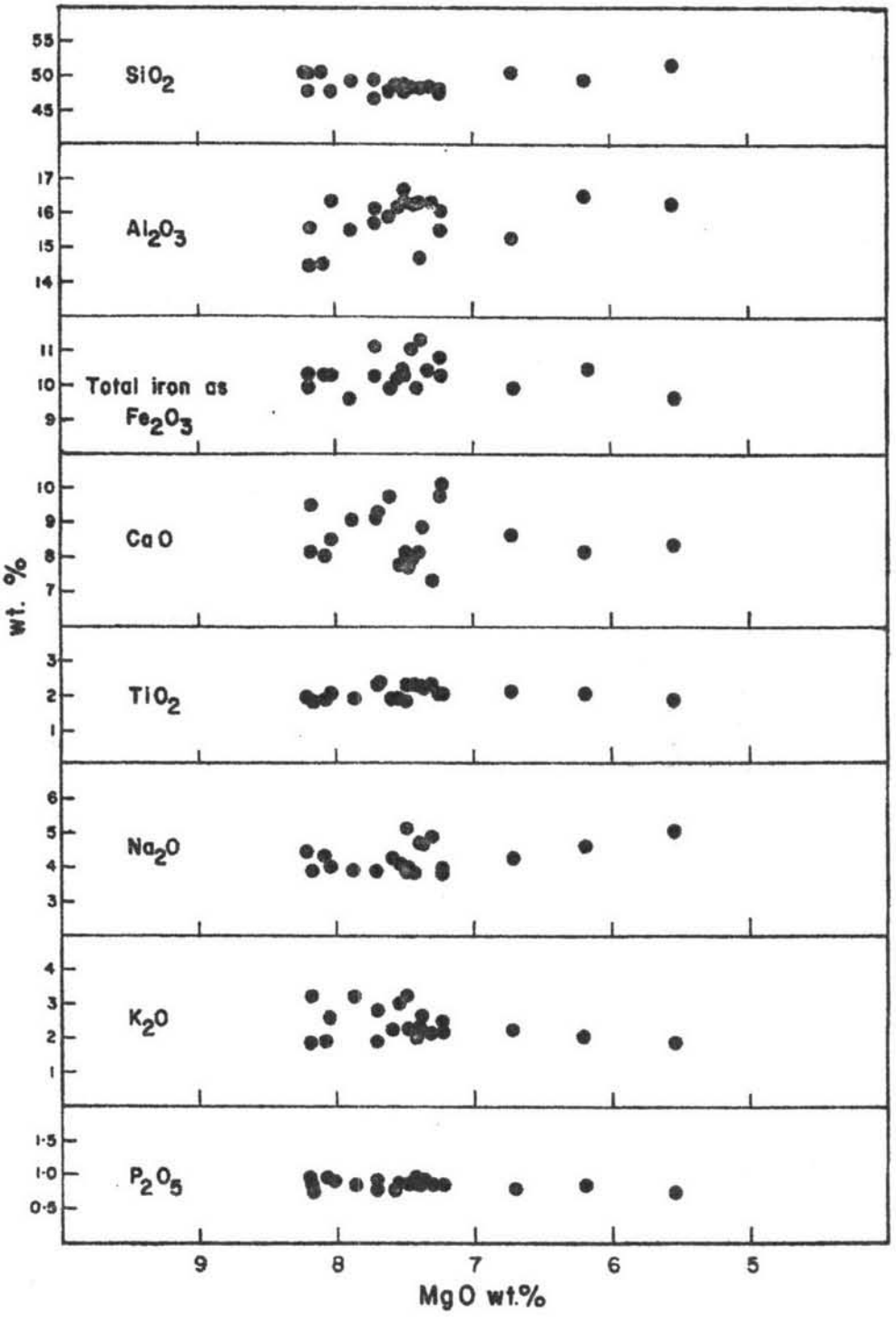

Figure 20 *MgO variation diagram demonstrating the extent of olivine control in the differentiation of the Bo-Phloi Basalt.*

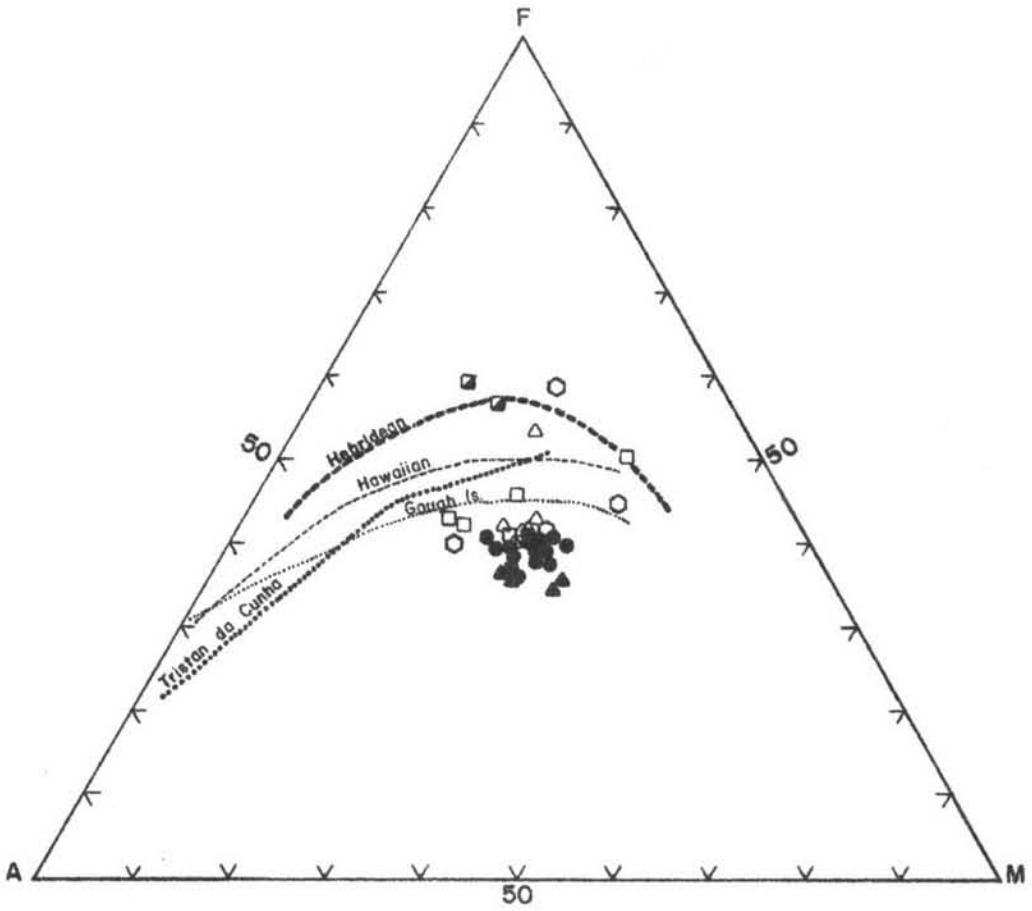

Figure 21 AFM diagram for the Bo Phloi Basalt. $A = Na_2O + K_2O$, $F = FeO + 0.8998\ Fe_2O_3$, $M = MgO$.

△ = Lampang basalts (1)

◪ = Wattana Nakhon basalts (1)

▲ = Lampang basalts (2)

○ = Khok Samrong basalts (2)

□ = BCK, SP, PS and S (2)

● = Bo-Phloi basalts

(1)..... from Vichit et. al., 1978

(2)..... from Barr and Macdonald, 1978

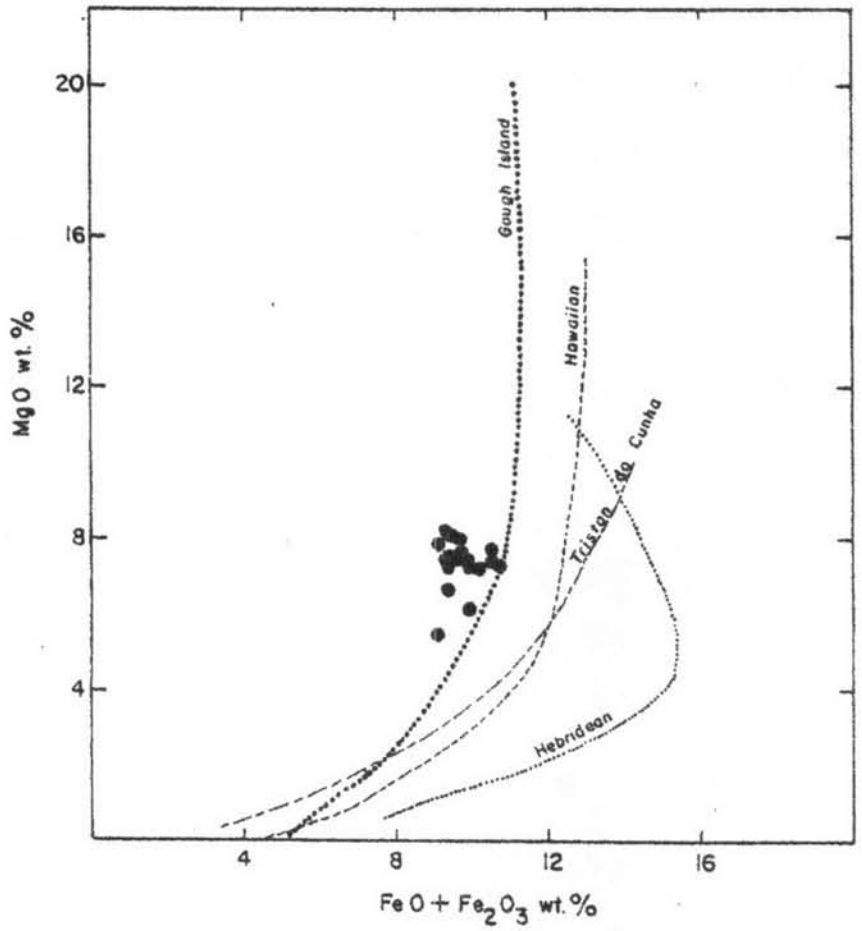

Figure 22 *MgO and $FeO + Fe_2O_3$ plot of the Bo-Phloi Basalt correrated to the generalized trends of the Hebridean alkalic, Hawaiian alkalic, Gough Island and Tristan da Cunha series (after Coombs and Wilkinson, 1969). Solid circles represent the Bo Phloi Basalt.*

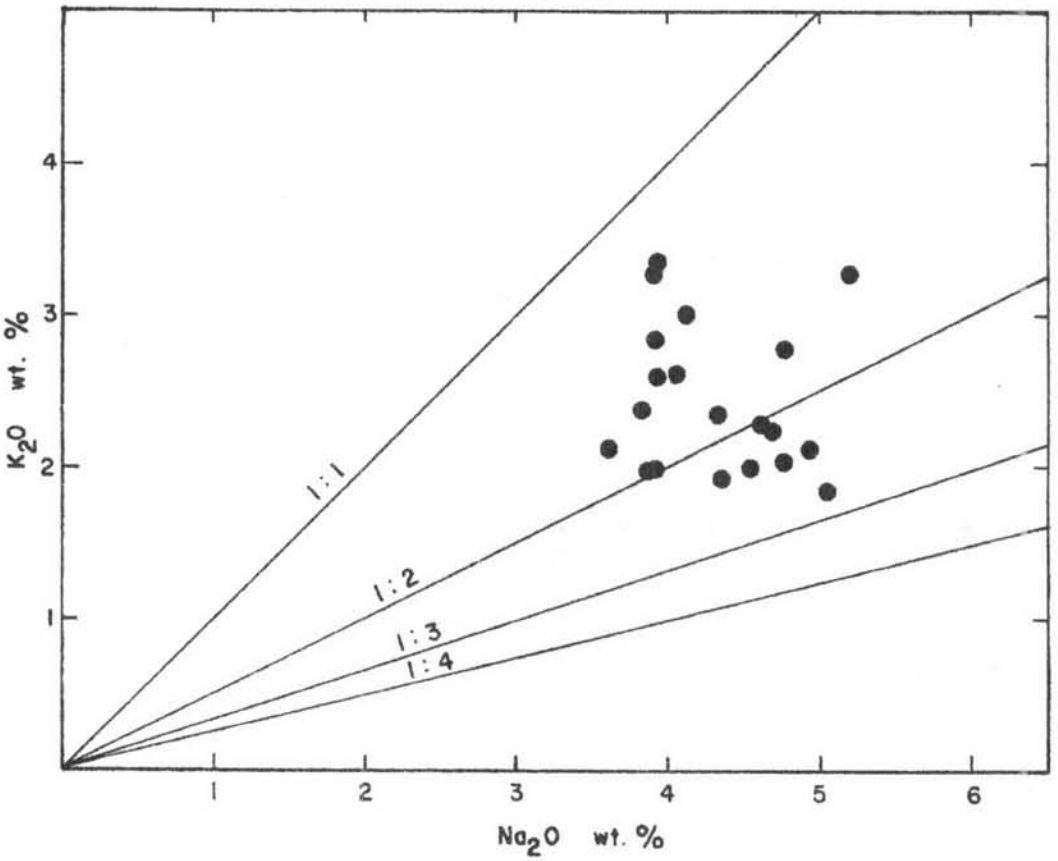

Figure 23 *Correlation of K_2O and Na_2O diagram for the Bo-Phlol Basalt.*

place the rocks into alkali basalt, the basanitic rock is exceeding prevalent over the alkali olivine basalt according to the classification of Yoder and Tilley (1962), and Green and Ringwood (1967). Total alkali ($Na_2O + K_2O$) vs SiO_2 diagram has been used as an aid in classifying the degree of alkalinity of the basalts (Macdonald and Katsura, 1964, and Kuno, 1968). Generally basaltic rocks are divided according to the alkali-silica diagram into alkaline and subalkaline (Irvine and Baragar, 1971). The alkaline portion is then subdivided into strongly alkaline and mildly alkaline series (Saggerson and Williams 1964). The former series contains modal nepheline whilst the latter contains no modal nepheline. The Bo-Phloi Basalt falls within the transition between strongly alkaline and mildly alkaline series (Figure 24). The K_2O/Na_2O ratio ranges from 0.37 to 0.84 and is principally greater than 1/2. This alkalic character is similar to those occurred in the Grand Canyon which is termed "Transitional basalts" (Best and Birmhall, 1974). Normative plagioclase composition (100 An/(An + Ab) ranges from 30 to 61 and is dominantly in between 40 to 50. This andesine normative plagioclase would replace hawaiite for alkali basalt for the Bo-Phloi Basalt (Macdonald, 1960).

Irvine and Baragar (1971) mentioned the two principal series of rocks in association with alkali olivine basalts (1) a "sodic series" of hawaiite-mugearite-benmorite-trachyte, common to the Hawaiian Island (Macdonald and Katsura, 1964; Macdonald, 1968) and Hebridean (Muir and Tilley, 1961) and (2) a "potassic series" of trachybasalt-tristanite-trachyte, typical of Tristan da Cunha (Baker et al., 1964) and Gough

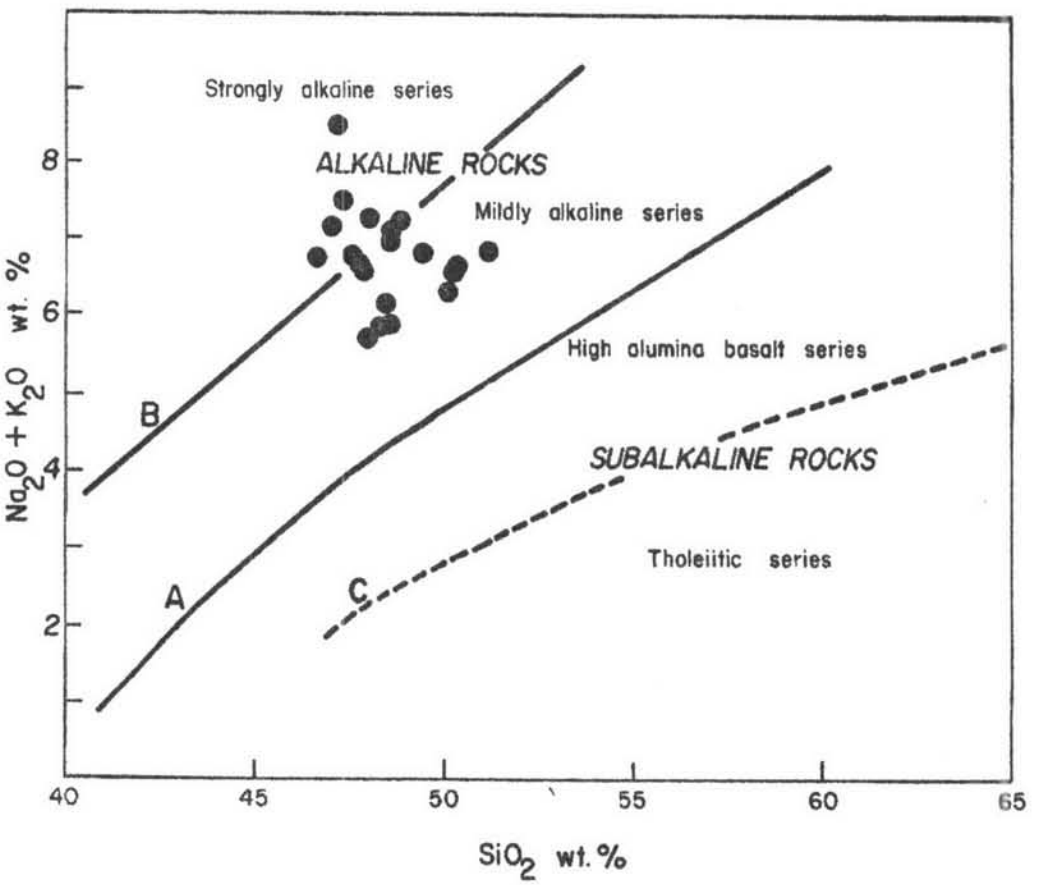

Figure 24 *Alkalies-silica diagram for the Bo-Phloi Basalt. Boundary lines are after Schwarzer and Rogers (1974).*

Line A - alkaline and subalkaline dividing line (Irvine and Baragar, 1971).
Line B - alkaline subdividing line (Saggerson and Williams, 1964).
Line C - subalkaline subdividing line (Kuno, 1968).

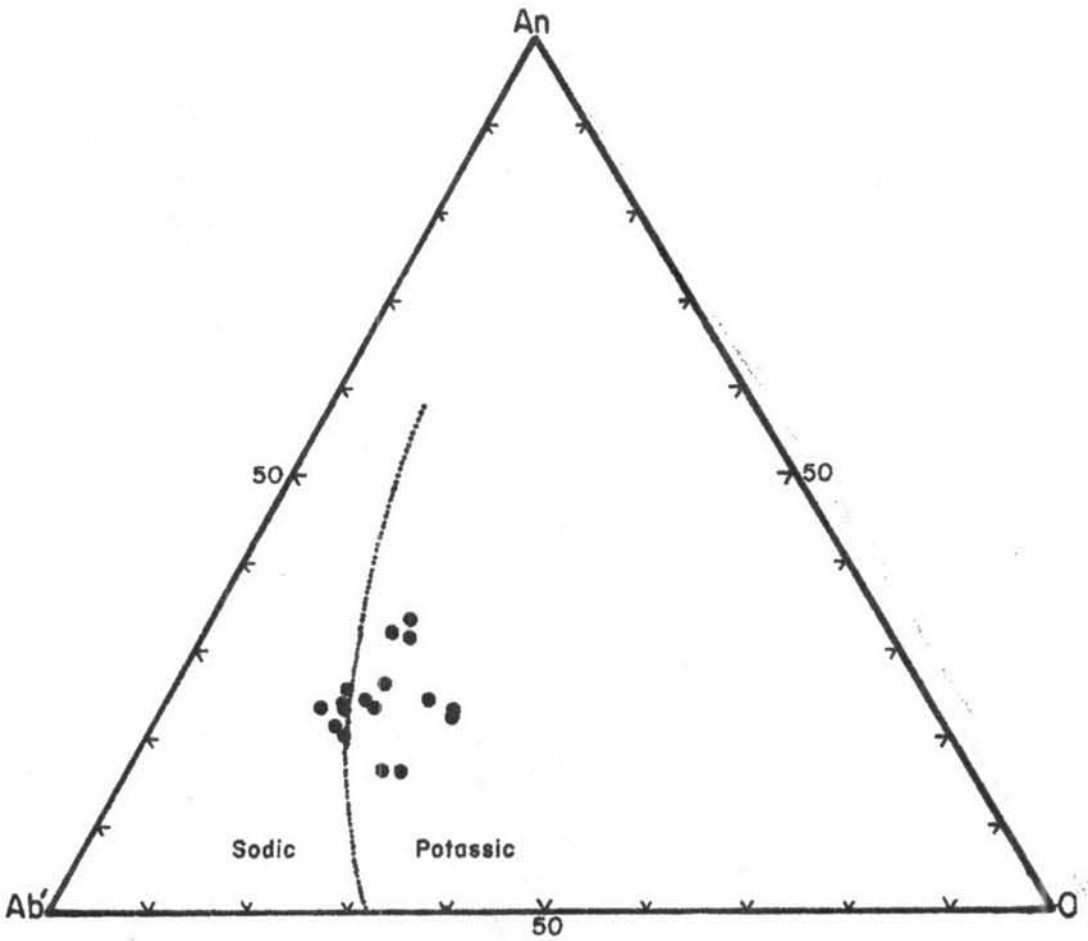

Figure 25 *An-Ab'-Or projections contrasting the two main alkali olivine basalt series. The dividing line is after Irvine and Baragar (1971). Solid circles represent the Bo-Phloi Basalt.*

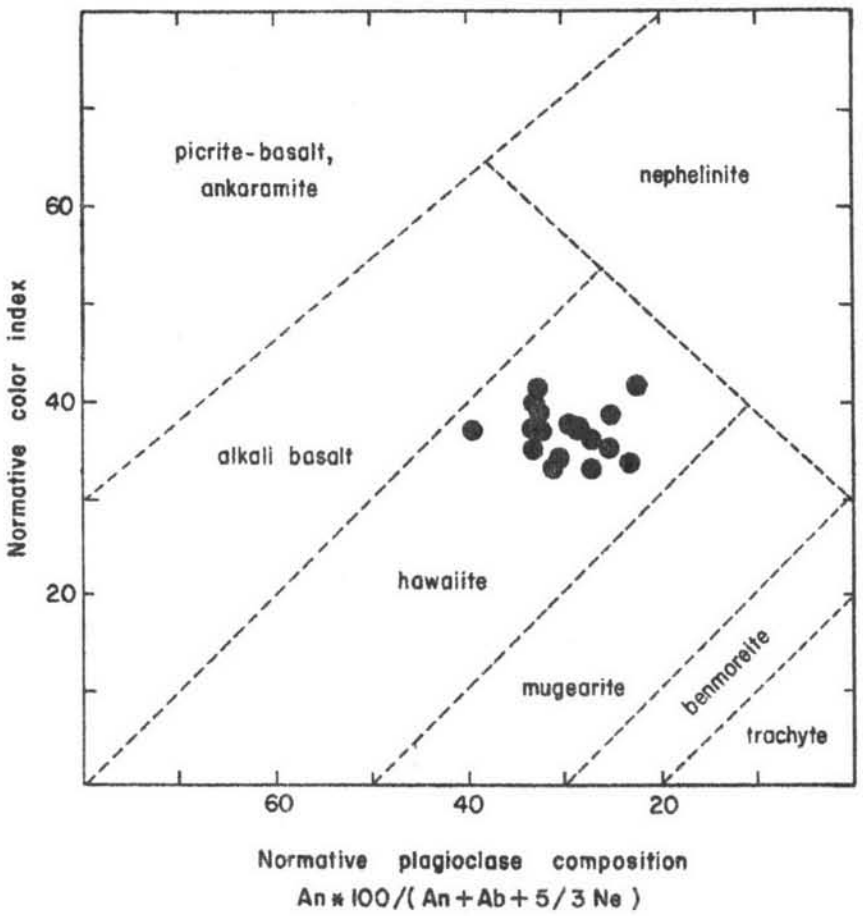

Figure 26 *Plot of normative color index versus normative plagioclase composition for the Bo-Phloi Basalt. Boundary lines are after Irvine and Baragar (1971).*

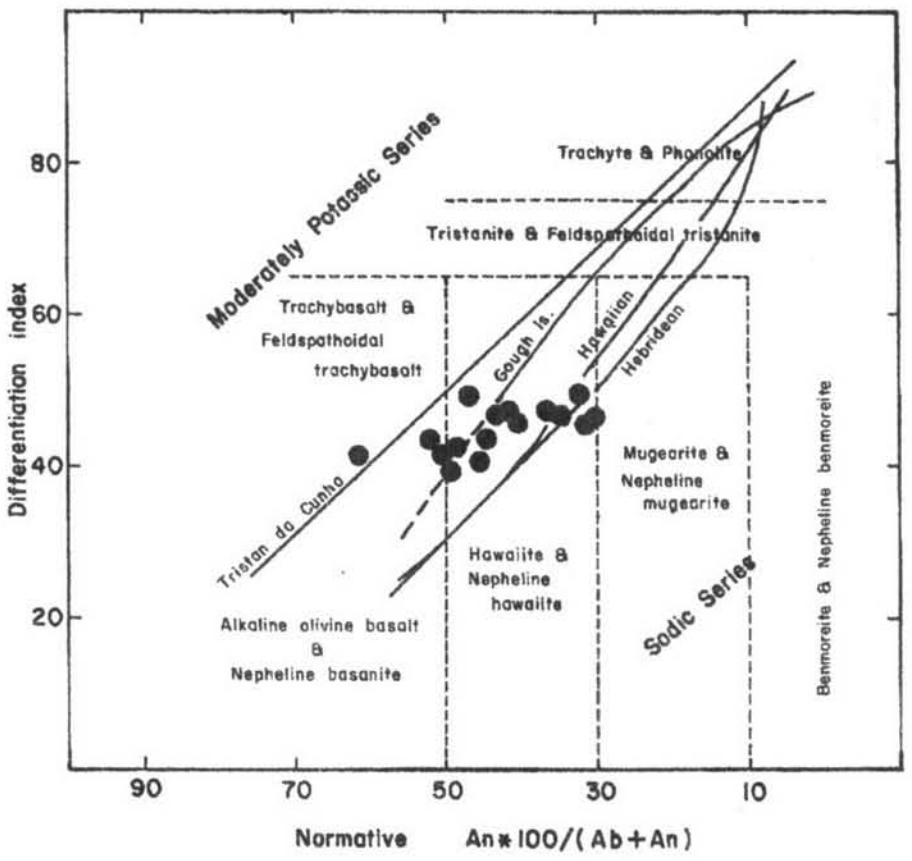

Figure 27 *Correlation of differentiation index and normative plagioclase composition for the Bo-Phloi Basalt. Nomenclature is after Coombs and Wilkinson (1969).*

Island (Le Maitre, 1962). They used the An-Ab'-Or projections for contrasting and subdividing these two main series, and an individual plot of normative color index versus normative plagioclase composition was constructed.

The plot of An-Ab'-Or diagram in Figure 25 illustrates that the Bo-Phloi Basalt lies comparatively well in potassic field. However, the K_2O content of the rocks (1.76 to 3.15 wt/%) is chemically too low to be considered as belonging to the potassic rock series. The Bo-Phloi Basalt should be placed on the sodic series with a moderate K-rich. The normative color index versus normative plagioclase composition diagram (Figure 26) classifies the Bo-Phloi Basalt as hawaiite. The correlation of differentiation index and normative plagioclase composition following the boundary lines of Coombs and Wilkinson (1969) also place the Bo-Phloi Basalt well within the Hawaiite field (Figure 27). These diagrams are going well with other characteristics i.e., alkalic character and normative composition of the rock.

Megacrysts

The Bo-Phloi alkaline basalt contains a large amount of unusually large crystals, quite distinct in sizes, habits and compositions. Chemical analyses of 9 pyroxene megacrysts and one each of olivine, sanidine and spinel megacrysts with structural formulae and end member formulae of these megacrysts are illustrated in Table 4.

Chemical analysis data of pyroxene megacrysts indicate to be Ca-rich clinopyroxene which is ranging in compositions from augite to

salite in pyroxene triangular diagram (Figure 28). Al-content in these pyroxene megacrysts is relatively high, leading to the high value of end member formulae of Ca-Tschermak molecule (approximately 30 percent). Atomic distribution of Al in terms of Al^{iv}/Al^{vi} is approximately 2. Mg-value of the pyroxene megacrysts, if calculated from the basis of $Fe_2O_3\% = TiO_2\ \% + 1.5$, would range from 82 to 87 with the average of 84. Plot of atomic proportions of Ti and Al^{iv} against Si in Figure 29 and plot of 100 Mg/(Mg+ΣFe) against TiO_2 weight percent in Figure 30 imply these clinopyroxene megacrysts tend to be grouped in the fields of those high-pressure clinopyroxenes from the Southern Highlands (N.S.W.), Australia and the Massif Central, France (Wass, 1979).

One chemical analysis of olivine megacryst shows that only three oxides, SiO_2, Fe_2O_3 (total iron) and MgO, are the major constituents. Others are either minor or almost absent. The end member formula of the olivine is Fo 87.5 : Fa 12.5 The Mg-value of olivine is 87.5, if the equation $Fe_2O_3\ \% = TiO_2\ \% + 1.5$ is assumed.

Chemical analysis of a spinel megacryst illustrates that the major constituents are Al_2O_3, Fe_2O_3, MgO and FeO. Atomic ratios calculated from the formula of spinel on the basis of O = 32.000 is pss shown in Table 4. The $R^{+2} : R^{+3}$ ratio is 1 : 2.16 and the atomic ratio of Mg : Fe^{2+} is 3.85 : 1.

One chemical analysis of sanidine megacryst from Vichit et al. (1978) shows four major constituents of SiO_2, Al_2O_3, Na_2O and K_2O. The Or-Ab-An (mole %)are plotted in feldspar triangular diagram (Figure 31).

Table 4 Chemical analyses of megacrysts from the Bo-Phloi Basalt.

	CPX-1	CPX-2	CPX-3
SiO_2	46.73	47.62	46.38
TiO_2	1.69	1.80	2.06
Al_2O_3	9.25	8.59	9.00
Fe_2O_3	2.97	3.33	4.19
FeO	3.57	3.49	3.46
MnO	0.11	0.10	0.11
MgO	13.21	13.48	12.55
CaO	20.04	19.92	20.30
Na_2O	0.95	1.02	1.10
H_2O^-	0.15	0.11	0.06
P_2O_5	0.02	0.01	0.01
Total	99.08	99.61	99.25
100 Mg/(Mg+ΣFe)	78.28	77.85	74.58
Mg-value	86.9	87.2	84.7
Structural formula on basis of 6 oxygens			
Si	1.74	1.76	1.73
Al^{iv}	0.26	0.24	0.27
Al^{vi}	0.14	0.13	0.12
Ti	0.05	0.05	0.06
Fe^{3+}	0.08	0.09	0.12
Fe^{2+}	0.11	0.11	0.11
Mn	0.003	0.003	0.004
Mg	0.73	0.74	0.70
Ca	0.80	0.79	0.81
Na	0.07	0.07	0.08
x + y	2.00	1.99	2.00
Atomic ratios			
Ca	46.24	45.47	46.66
Mg	42.36	42.82	40.15
$Fe^{3+}+Fe^{2+}+Mn$	11.40	11.71	13.19
Al^{iv}/Al^{vi}	1.81	1.83	2.21
End members	$Tsch_{29}Ac-Jd_8$ $-Hd_{11}Di_{52}$	$Tsch_{28}AcJd_7$ $-Hd_{11}Di_{54}$	$Tsch_{30}Ac+Jd_8$ $-Hd_{11}Di_{51}$
or	$Ac+Jd_{16}Hd_{16}Di_{73}$	$Ac+Jd_{10}Hd_{15}Di_{75}$	$Ac+Jd_{12}Hd_{16}Di_{72}$

Table 4 (continued)

	CPX-4	CPX-5	CPX-6
SiO_2	46.60	46.27	46.09
TiO_2	2.04	2.09	1.95
Al_2O_3	8.45	8.75	9.29
Fe_2O_3	4.11	4.61	4.60
FeO	3.76	3.77	3.80
MnO	0.12	0.11	0.12
MgO	12.92	12.06	12.02
CaO	20.04	20.27	20.21
Na_2O	1.11	1.16	1.16
H_2O^-	0.04	0.18	0.21
P_2O_5	0.01	0.01	0.02
Total	99.23	99.31	99.49
100 Mg/(Mg+ΣFe)	74.65	71.87	71.81
Mg-value	84.4	82.1	81.6
Structural formulae on basis of 6 oxygens			
Si	1.74	1.73	1.72
Al^{iv}	0.26	0.27	0.28
Al^{vi}	0.11	0.12	0.13
Ti	0.06	0.06	0.06
Fe^{3+}	0.12	0.13	0.13
Fe^{2+}	0.12	0.12	0.12
Mn	0.004	0.004	0.004
Mg	0.72	0.67	0.67
Ca	0.80	0.81	0.81
Na	0.08	0.08	0.08
x + y	2.00	2.00	2.00
Atomic ratios			
Ca	45.64	46.77	46.84
Mg	40.91	38.71	38.74
$Fe^{3+}+Fe^{2+}+Mn$	13.45	14.52	14.42
Al^{iv}/Al^{vi}	2.40	2.35	2.12
End members	$Tsch_{29}Ac+Jd_8$ $-Hd_{12}Di_{51}$	$Tsch_{29}Ac+Jd_8$ $-Hd_{12}Di_{51}$	$Tsch_{31}Ac+Jd_9$ $-Hd_{12}Di_{48}$
or	$Ac+Jd_{11}Hd_{17}Di_{72}$	$Ac+Jd_{12}Hd_{17}Di_{71}$	$Ac+Jd_{12}Hd_{18}Di_{70}$

Table 4 (continued)

	CPX-7	CPX-8	CPX-9
SiO_2	45.82	48.67	46.15
TiO_2	1.95	1.05	1.87
Al_2O_3	9.60	8.49	9.40
Fe_2O_3	3.72	2.56	3.70
FeO	3.68	5.23	4.04
MnO	0.11	0.11	0.11
MgO	12.66	15.15	13.01
CaO	20.35	16.07	19.20
Na_2O	1.12	1.51	1.16
H_2O^-	0.18	0.18	0.08
P_2O_5	0.01	nil	0.01
Total	99.22	99.05	98.76
100 Mg/(Mg+ΣFe)	75.30	77.69	74.94
Mg-value	85.5	83.8	84.2
Structural formulae on basis of 6 oxygens			
Si	1.71	1.80	1.73
Al^{iv}	0.29	0.20	0.27
Al^{vi}	0.13	0.17	0.14
Ti	0.05	0.03	0.05
Fe^{3+}	0.11	0.07	0.10
Fe^{2+}	0.12	0.16	0.13
Mn	0.003	0.004	0.004
Mg	0.70	0.83	0.73
Ca	0.81	0.64	0.77
Na	0.08	0.11	0.08
x + y	2.01	2.01	2.01
Atomic ratios			
Ca	46.70	37.27	44.50
Mg	40.39	48.88	41.96
$Fe^{3+}+Fe^{2+}+Mn$	12.91	13.85	13.54
Al^{iv}/Al^{vi}	2.18	1.24	1.98
End members	$Tsch_{32}Ac+Jd_8$ $-Hd_{12}Di_{48}$	$Tsch_{24}Ac+Jd_{11}$ $-Hd_{17}Di_{48}$	$Tsch_{31}Ac+Jd_8$ $-Hd_{13}Di_{48}$
or	$Ac+Jd_{12}Hd_{17}Di_{71}$	$Ac+Jd_{14}Hd_{22}Di_{64}$	$Ac+Jd_{12}Hd_{19}Di_{69}$

Table 4 (continued)

	SP	SA	OL
SiO_2	2.76	62.54	39.92
TiO_2	0.87	0.05	1.11
Al_2O_3	56.34	21.13	0.40
Fe_2O_3	10.54	0.12	2.61
FeO	8.44	0.82	10.60
MnO	0.08	0.01	n.d.
MgO	18.35	0.16	41.70
CaO	1.42	1.02	0.42
Na_2O	nil	5.13	< 0.1
K_2O	0.02	8.73	< 0.1
H_2O^-	0.15	0.06	n.d.
P_2O_5	nil	0.16	0.20
Cr_2O_3	0.05	0.01	n.d.
NiO	0.09	n.d.	n.d.
Total	99.71	99.99	96.98
Structural formula on basis of 32 oxygens, 4 oxygens			
Si	0.57	11.03	1.02
Al	13.76	4.40	0.01
Ti	0.14	0.01	0.02
Cr	0.01	n.d.	n.d.
Fe^{3+}	1.64	0.02	0.05
Fe^{2+}	1.46	0.12	0.23
Mn	0.01	0.001	n.d.
Ni	0.01	n.d.	n.d.
Mg	5.67	0.04	1.58
Ca	0.31	0.19	0.01
Na	nil	1.76	0.001
K	nil	1.97	0.001
	atomic ratio	mole %	atomic ratio
	$R^{2+} : R^{3+} = 1 : 2.2$	Or : Ab : An	Fo . Fa = 87.5 : 12.5
	$Mg : Fe^{2+} = 3.8 : 1$	50.3 : 44.8 : 4.9	

Remarks : chemical analyses of CPX-1 to CPX-9 and SP are megacrysts of clinopyroxene and spinel, respectively ; and are analyzed by Mrs. Pranee Choosri Geological Survey Division, Department of Mineral Resources

chemical analysis of SA - sanidine megacryst, is from Vichit et al., 1978

chemical analysis of OL - olivine megacryst, is done by Dr. Wasant Pongsapich

all clinopyroxene megacrysts include 0.01 wt% Cr_2O_3 but except for sample CPX-1 contains 0.07 wt%

sample CPX-1, CPX-3, CPX-4 and CPX-5 include 0.02 wt% K_2O, the others contain 0.01 wt% K_2O

sample CPX-1, CPX-2, CPX-8 and CPX-9 include 0.34, 0.12, 0.01 and 0.01 wt% NiO, respectively

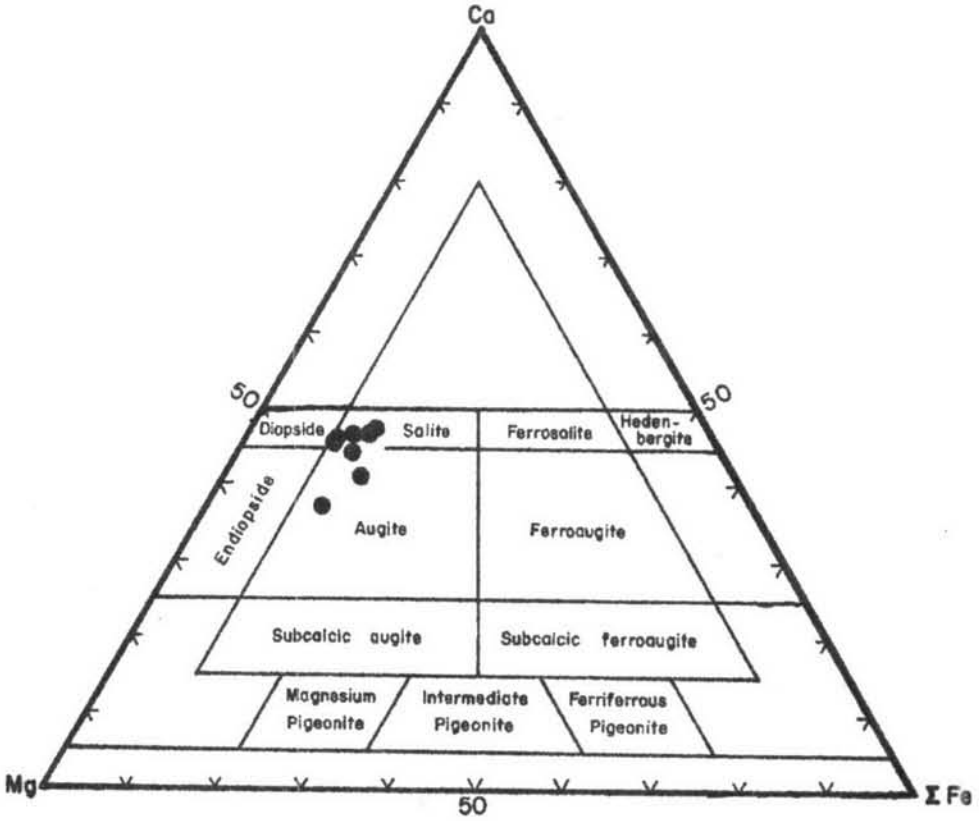

Figure 28 *Compositions of pyroxene megacryst from the Bo-Phloi Basalt. Boundary lines are after Deer, Howie and Zussman (1963).*

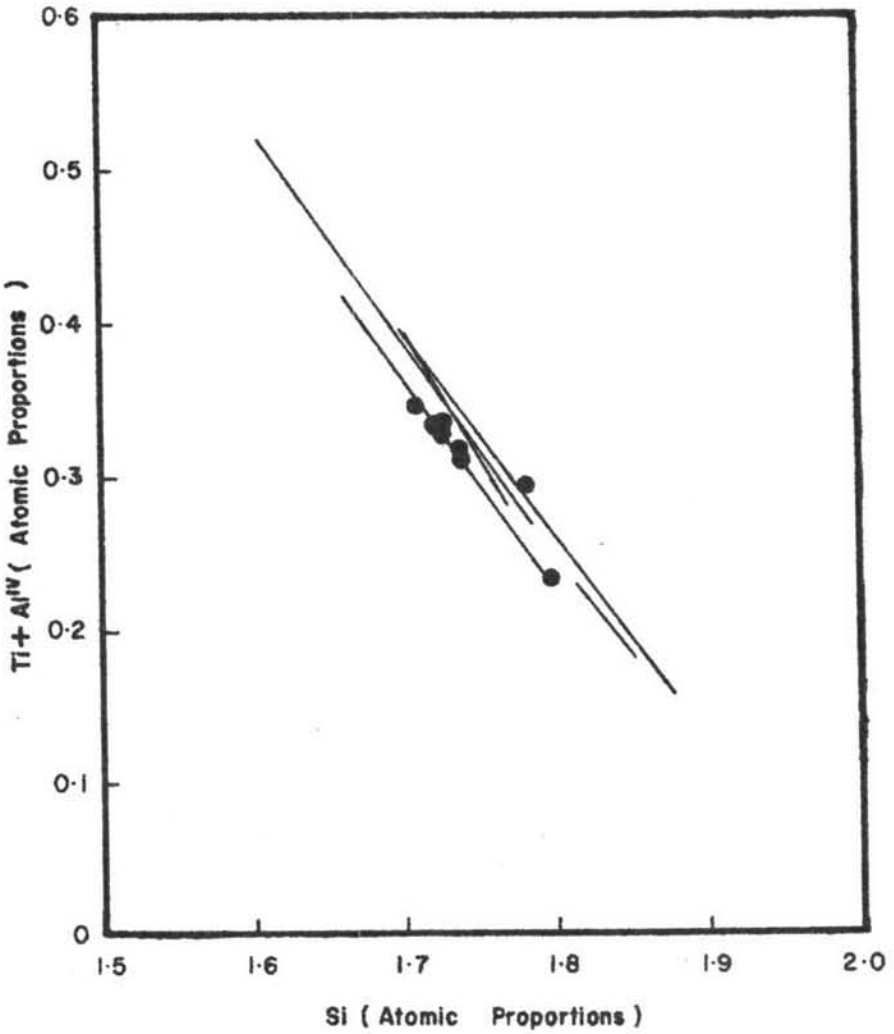

Figure 29 *Plot of atomic proportions of Ti and Al^{IV} against Si for clinopyroxene megacrysts from the Bo-Phloi Basalt. Tie lines join cognate high-pressure and low-pressure clinopyroxenes from the Southern Highlands, N.S.W. and the Massif Central, France (after Wass, 1979).*

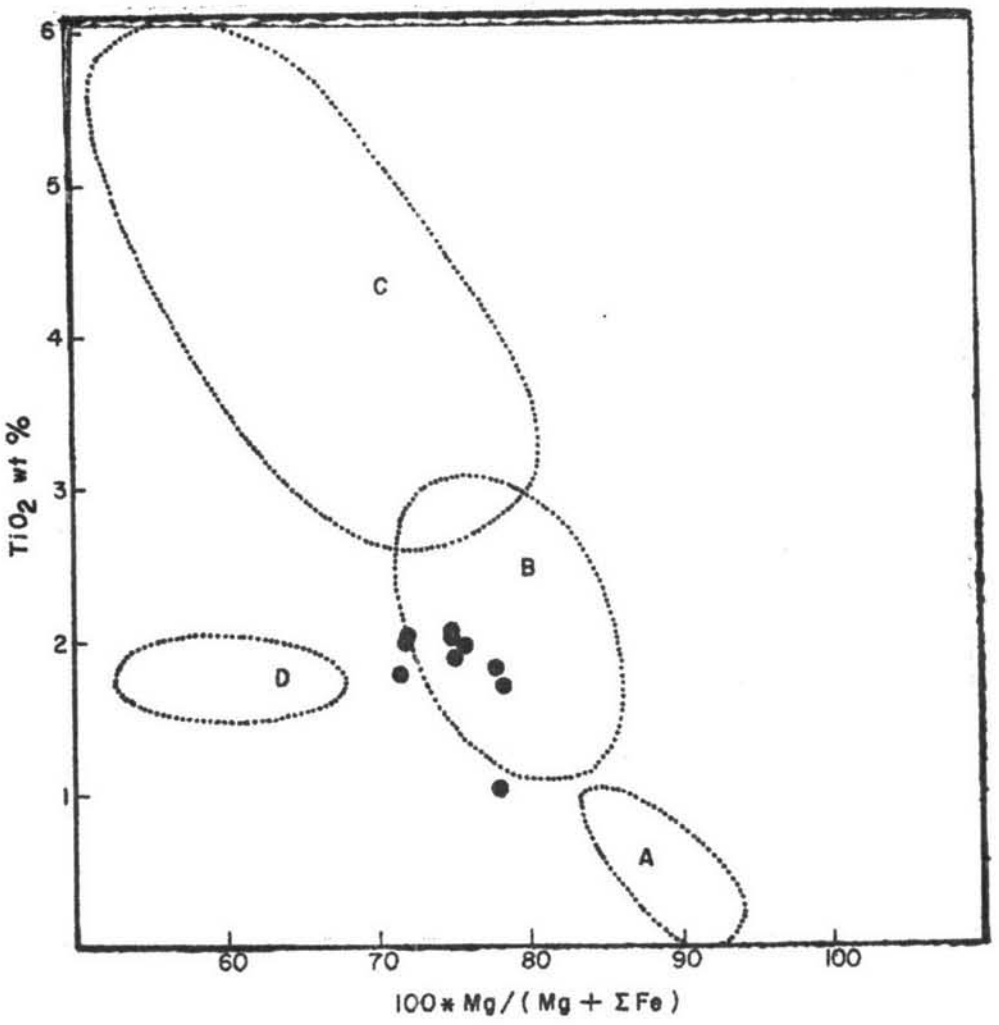

Figure 30 *Variation in $100*Mg/(Mg+\Sigma Fe)$ with TiO_2 weight percent of clinopyroxene megacrysts from the Bo-Phloi Basalt. Circles A, B, C and D outline the fields of densest concentration of clinopyroxenes of origins 1, 2, 3 and 4 respectively (after Wass , 1979).*

Remarks :–

Origin 1 : Cr-diopsides which are accidentally-included mantle xenoliths.

Origin 2 : Al-augites from accidentally-included xenoliths of basaltic compositions which had crystallised in the mantle from a previous melting episode.

Origin 3 : Al-augites, as discrete megacrysts or in xenoliths representing high-pressure crystallisation products of alkali basaltic melts which were probably contemporaneous with magmatic events producing the host rocks. A cognate relationship is established where multiple overgrowths are developed.

Origin 4 : Phenocryst and quench clinopyroxenes which crystallised at low pressure and thus show no reaction and rimming relationships.

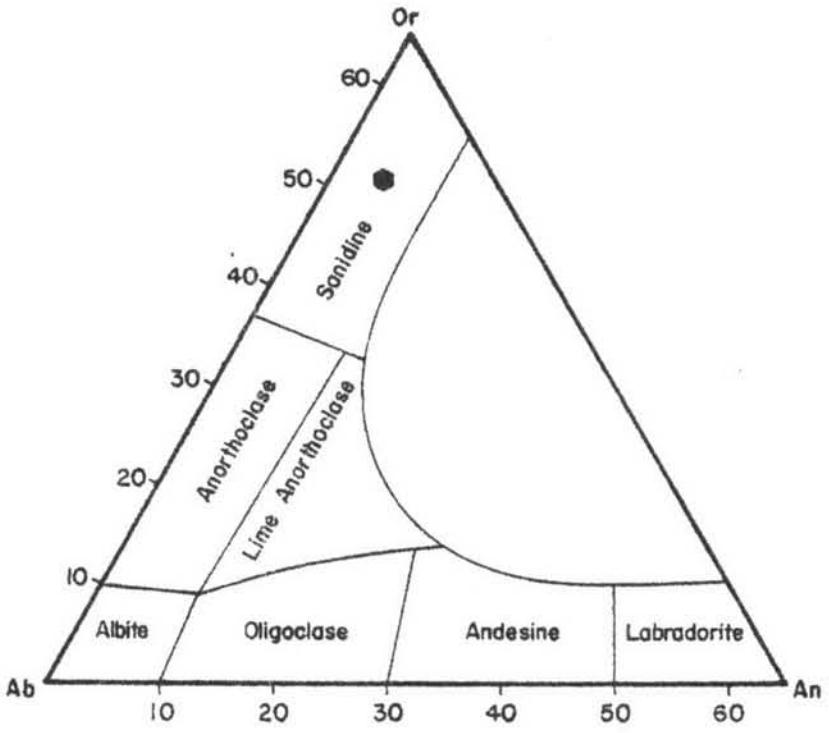

Figure 31 *Plot of Ab-Or-An (mole percent) for a sanidine megacryst from the Bo-Phloi Basalt. Boundary lines are after Irving, 1974 b.*

Ultramafic Nodules

Bo-Phloi ultramafic nodules or inclusions are commonly lherzolite, which contain the mineral assemblages of olivine-orthopyroxene-clinopyroxene-spinel. Their chemical compositions and the MgO/ΣFeO ratios are presented in Table 5. They are rather rich in the lower melting components. The plots of oxides against MgO/ΣFeO ratios in Figure 32, demonstrated that most of the lower melting components such as CaO, $Na_2O + K_2O$ and TiO_2 increase with decreasing MgO/ΣFeO ratios where as MgO striking decreases. The plots are well within the general limits of variations of lherzolite nodules (Kuno and Aoki, 1970, Figure 3). These Bo-Phloi ultramafic inclusions are lherzolite, chemically.

Table 5 Chemical compositions of lherzolite nodules from the Bo-Phloi Basalt.

	T79-6-2	T79-7-2	T79-7-3
SiO_2	43.76	42.99	42.43
TiO_2	0.20	0.15	0.14
Al_2O_3	4.50	3.41	3.55
Fe_2O_3	1.01	1.16	0.82
FeO	6.77	6.99	7.12
MnO	0.13	0.15	0.12
MgO	32.50	37.25	40.83
CaO	8.44	5.61	2.41
Na_2O	0.30	0.19	0.15
K_2O	0.08	0.09	0.08
H_2O^-	0.37	0.36	0.37
Loss on ignition	0.59	0.83	0.73
P_2O_5	0.02	0.01	0.01
Cr_2O_3	0.20	0.20	0.20
Total	98.87	99.39	98.96
$MgO/(FeO+Fe_2O_3 x 0.9)$	4.23	4.64	5.20
Mg-value	89.50	90.50	91.10

Remarks : chemical analyses are done by Ms. Pranee Choosri, Geological Survey Division, Department of Mineral Resources.

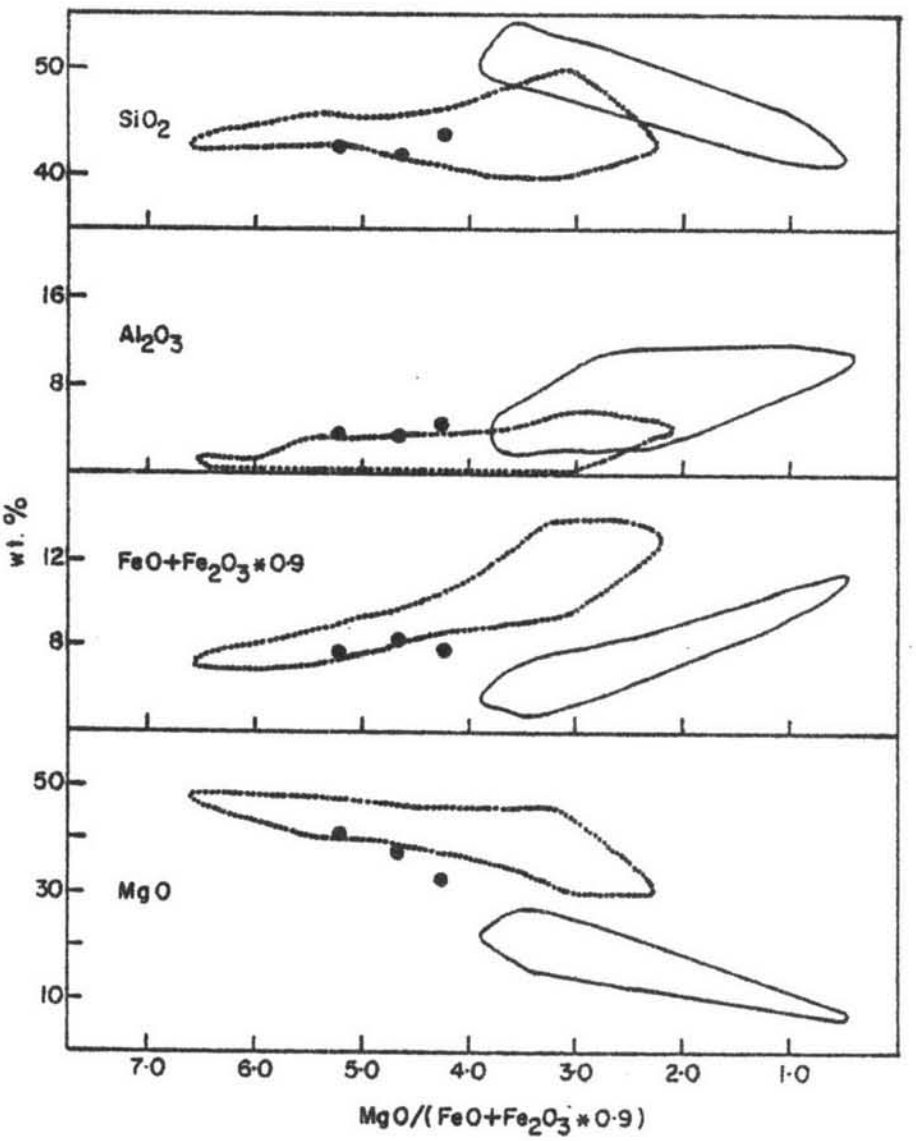

Figure 32 *Weight per cents of oxide components of ultramafic nodules in the Bo-Phloi Basalt plotted against MgO/ΣFeO (weight). The closed broken curves mark the general limit of variation of lherzolite nodules. The closed solid curves mark the limit of variation of pyroxenite nodules (Kuno and Aoki, 1970).*

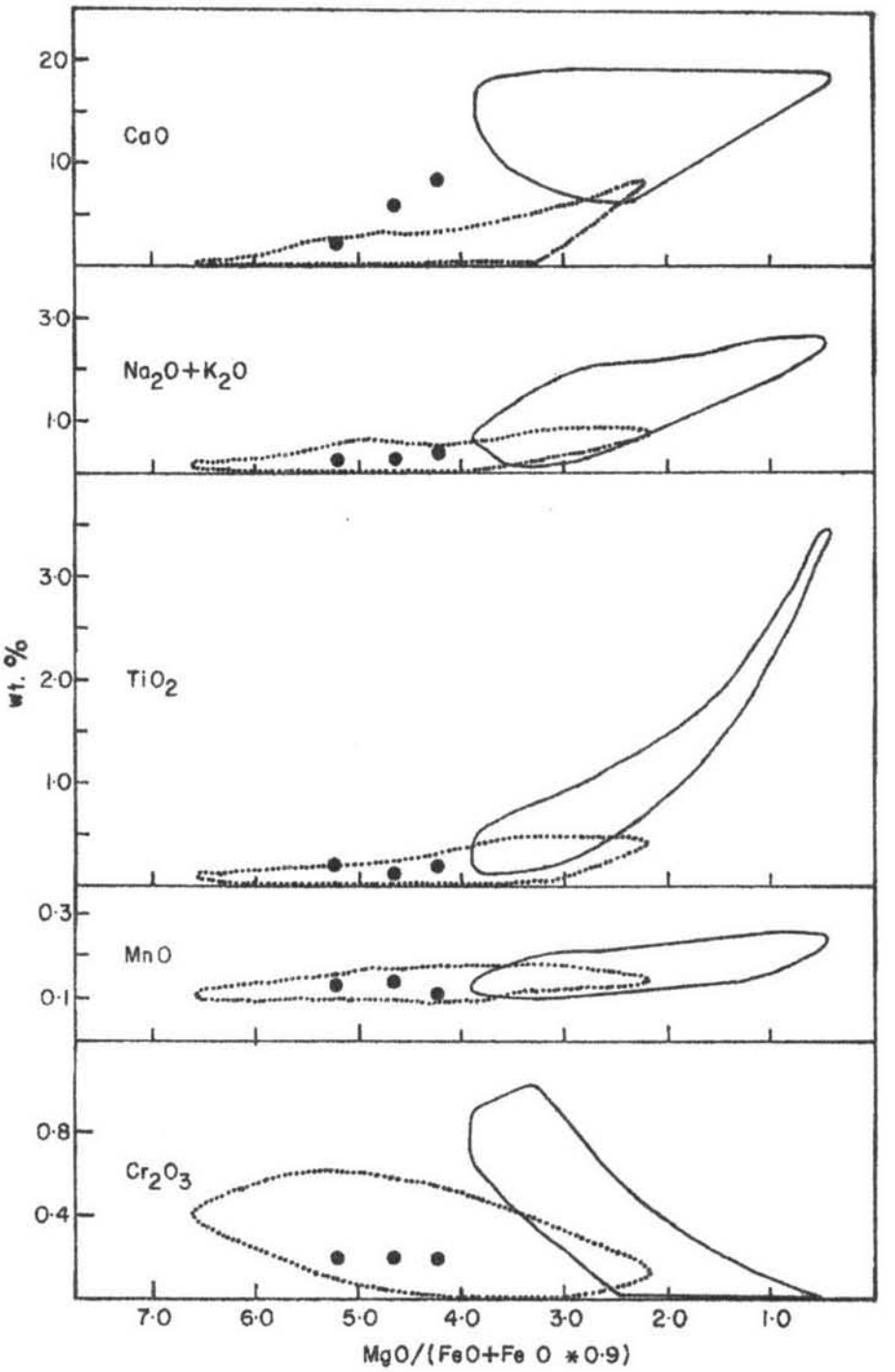

Figure 32 *(continued)*